20 August 1998

PHYSICS LETTERS B

ELSEVIER

Physics Letters B 434 (1998) 180–188

Study of the isovector scalar mesons in the channel $\bar{p}p \to K^{\pm}K^{0}_{S}\pi^{\mp}$ at rest with initial angular momentum state selection

OBELIX Collaboration

A. Bertin [a], M. Bruschi [a], M. Capponi [a], S. De Castro [a], R. Dona' [a], A. Ferretti [a], D. Galli [a], B. Giacobbe [a], U. Marconi [a], M. Piccinini [a], M. Poli [a,1], N. Semprini Cesari [a],R. Spighi [a], V. Vagnoni [a], S. Vecchi [a], F. Vigotti [a], M. Villa [a], A. Vitale [a], A. Zoccoli [a], A. Benedettini [a], E. Lodi Rizzini [b], A. Zenoni [b], L. Venturelli [b],M. Corradini [b], A. Donzella [b], C. Cicalo' [c], A. Masoni [c], S. Mauro [c], G. Puddu [c],S. Serci [c], P. Temnikov [c,2], G. Usai [c], O.E. Gorchakov [d], S.N. Prakhov [d],A.M. Rozhdestvensky [d], M.G. Sapozhnikov [d], V.I. Tretyak [d], P. Gianotti [e],C. Guaraldo [e], A. Lanaro [e], V. Lucherini [e], F. Nichitiu [e,3], C. Petrascu [e,3], A. Rosca [e,3],V. Ableev [f,4], C. Cavion [f], U. Gastaldi [f], M. Lombardi [f], G. Maron [f], R.A. Ricci [f],G. Vedovato [f], G. Bendiscioli [g], V. Filippini [g], A. Fontana [g], P. Montagna [g], A. Rotondi [g],A. Saino [g], P. Salvini [g], C. Scoglio [g], M. Agnello [h,5], F. Balestra [h], E. Botta [h],T. Bressani [h], M.P. Bussa [h], L. Busso [h], P. Cerello [h], D. Calvo [h], S. Costa [h],O. Denisov [h,6], D. D'Isep [h], A. Feliciello [h], L. Ferrero [h], A. Filippi [h], R. Garfagnini [h],A. Grasso [h], F. Iazzi [h,5], A. Maggiora [h], S. Marcello [h], B. Minetti [h,5], D. Panzieri [h], E. Rossetto [h], F. Tosello [h], L. Valacca [h], G. Zosi [h], G. Pauli [i], S. Tessaro [i], L. Santi [j]

[a] *Dipartimento di Fisica, Universita' di Bologna and INFN, Sez. di Bologna, Bologna, Italy*
[b] *Dipartimento di Chimica e Fisica per l'Ingegneria e per i Materiali, Universita' di Brescia and INFN Sezione di Pavia, Pavia, Italy*
[c] *Dipartimento di Fisica, Universita' di Cagliari and INFN, Sezione di Cagliari, Cagliari, Italy*
[d] *Joint Institute of Nuclear Research, Dubna, Moscow, Russia*
[e] *Laboratori Nazionali di Frascati dell' INFN, Frascati, Italy*
[f] *Laboratori Nazionali di Legnaro dell' INFN, Legnaro, Italy*
[g] *Dipartimento di Fisica Nucleare e Teorica, Universita' di Pavia and INFN, Sezione di Pavia, Pavia, Italy*
[h] *Istituto di Fisica, Universita' di Torino and INFN, Sez. di Torino, Torino, Italy*
[i] *Istituto di Fisica, Universita' di Trieste and INFN, Sez. di Trieste, Trieste, Italy*
[j] *Istituto di Fisica, Universita' di Udine and INFN, Sez. di Trieste, Trieste, Italy*

Received 24 April 1998; revised 31 May 1998
Editor: L. Montanet

PII: S0370-2693(98)00767-9

Abstract

The study of the $I=1, J^{PC}=0^{++}$ states with the OBELIX detector in the channel $\bar{p}p \to K^{\pm}K^{0}_{S}\pi^{\mp}$ at three different target densities is reported. The data show the evidence for an extra scalar state with mass 1.29 ± 0.01 GeV$/c^2$ and width 0.080 ± 0.005 GeV$/c^2$.

The identification of the isovector member of the scalar nonet is a very important step in the search for the scalar glueball since its mass and width would provide the natural mass and width scale for the singlet member of the nonet and allows to discriminate among different theoretical models. This can provide the means to identify a resonance as an ordinary $\bar{q}q$ meson or a possible glueball candidate.

The channel $\bar{p}p \to K^{\pm}K^{0}_{S}\pi^{\mp}$ is ideal to study isovector scalar mesons since $I=0$, $J^{PC}=0^{++}$ states are not present.

The first measurement of that channel was performed at CERN in 1967 in antiproton-proton annihilation at rest in liquid hydrogen [1]. About 2000 events with negligible background were isolated and a spin parity analysis was performed within the isobar model neglecting the $\bar{p}p$ $P-wave$ contribution. Evidence of the following intermediate states was reported: K^{*} from the $I=0$ and $I=1$ $\bar{p}p$ states; $K\pi$ S wave interactions, described in the scattering length approximation; $a_0(980)$, described by a Breit-Wigner function with mass ~ 1.0 GeV$/c^2$ and width ~ 0.09 GeV$/c^2$; $a_2(1320)$, with mass 1.28 GeV$/c^2$ and width 0.09 GeV$/c^2$. No other scalar state was required.

In this paper we report on the study of the channel $K^{\pm}K^{0}_{S}\pi^{\mp}$ from $\bar{p}p$ annihilations at rest at three different hydrogen target densities: liquid hydrogen (LH_2, $\sim 90\%$ S wave); gaseous hydrogen at NTP (NTP, $\sim 50\%$ S wave); low pressure (5 mbar) hydrogen gas (LP, $\sim 10\%$ S wave).

Indeed, with very low pressure ($\sim$ mbar) hydrogen targets, antiprotons annihilate predominantly from P wave. By increasing the pressure, the S/P wave ratio increases because of the Stark mixing among levels. This effect is known as the Day-Snow-Sucher mechanism [2].

The selection of the $\bar{p}p$ initial state is a very valuable tool in meson spectroscopy both for the understanding of the resonance production mechanisms as well as for disentangling nearby resonances featuring different J^{PC}. The possibility to operate an initial state selection by changing the target density is a unique feature of the OBELIX apparatus [3].

In this work we present a simultaneous spin-parity analysis of the three data samples. The main result is the indication of the presence of a scalar resonance with mass around 1.29 GeV$/c^2$ and width of about 0.08 GeV$/c^2$. Moreover, the production of $a_0(980)$ is observed from the $^1S_0$ $\bar{p}p$ initial state only.

The experiment was performed at the Low Energy Antiproton Ring (LEAR) at CERN, using the OBELIX apparatus [4]. A complex system of different targets was developed to operate at different target densities from gaseous hydrogen at a few mbar to liquid hydrogen [3].

In Table 1 the number of collected annihilations and the number of events accepted after the selection cuts are shown for the three data sets. These samples are much bigger than those collected by all previous experiments (4 to 10 times).

The selection criteria were common to all data samples. The trigger was based on time-of-flight (TOF) information. It required four scintillator hits both in the internal and in the external barrel plus at least one track with a time-of-flight >8 ns. The latter condition is required in order to enrich the number of events containing charged kaons.

[1] Dipartimento di Energetica ''Sergio Stecco'',Universita' di Firenze, Firenze, Italy.

[2] On leave of absence from Institute for Nuclear Research and Nuclear Energy, Sofia, Bulgaria.

[3] On leave of absence from National Institute of Research and Development for Physics and Nuclear Engineering ''Horia Hulubei'', Bucharest-Magurele, Romania.

[4] On leave from Joint Institute of Nuclear Research, Dubna, Moscow, Russia.

[5] Politecnico di Torino and INFN, Sez. di Torino, Torino, Italy.

[6] On leave of absence from Joint Institute of Nuclear Research, Dubna, Moscow, Russia.

Table 1
Summary of the collected statistics

Target	$N_{\bar{p}}$	$N_{K^\pm K_S^0 \pi^\pm}$
LH_2	$1.7 \cdot 10^7$	$10.9 \cdot 10^3$
NTP	$2.4 \cdot 10^7$	$27.7 \cdot 10^3$
LP	$6.0 \cdot 10^6$	$3.0 \cdot 10^3$

Events with four reconstructed charged particles and zero net charge were first selected. Quality cuts on the χ^2 of the track fitting ($\chi^2/\text{track} < 3$) and single track momentum resolution ($\sigma_p/p < 0.2$) were applied. Particles were identified by TOF (when measured) and dE/dx; the selection criteria were tuned in order to achieve a smooth and high efficiency in kaon and pion identification ($> 80\%$), and a very low pion contamination in kaon identification (about 0.3%). The K_S^0 was reconstructed through mass identification in the $\pi^+\pi^-$ decay. The combinatorial background in the K_S^0 reconstruction turned out to be about a few percents with no influence on the analysis results. We then applied a selection by 5C kinematic fit with a selection cut on χ^2 corresponding to 90% confidence level.

The most important background source is the $\pi^+\pi^-\pi^+\pi^-\pi^0$ annihilation channel, in which a charged pion is misidentified as a kaon and two charged pions reconstruct the K_S^0 mass. In order to understand the effect of this background we simulated a sample of 5π events and submitted it to the same analysis chain used for the identification of the $K^\pm K_S^0 \pi^\mp$ channel. We found a rejection factor of about 3×10^5. Even though the annihilation frequency for the 5π channel is 10^3 times higher than that of $K^\pm K_S^0 \pi^\mp$ (see Table 2) the contamination turned out to be negligible.

Annihilation frequencies in the three samples were evaluated by normalizing the production rate of the $K^\pm K_S^0 \pi^\mp$ channel to the $\pi^+\pi^-\pi^+\pi^-\pi^0$ channel. The 5π annihilation frequency has been measured for LH_2 and NTP targets in a previous paper [5] and did not show any dependence on the target density. The measured value was: $r_{5\pi} = (17.84 \pm 0.35) \cdot 10^{-2}$ and it was used also for the LP sample. The $K^\pm K_S^0 \pi^\mp$ annihilation frequency is calculated as:

$$r_{K\bar{K}\pi} = \frac{N_{K^\pm K_S^0 \pi^\mp}}{N_{5\pi}(1 - b_{5\pi})} \frac{\epsilon_{5\pi}}{\epsilon_{K^\pm K_S^0 \pi^\mp}} r_{5\pi},$$

where $N_{K^\pm K_S^0 \pi^\mp}$ and $N_{5\pi}$ are the numbers of $K^\pm K_S^0 \pi^\mp$ and 5π events, respectively; $\epsilon_{K^\pm K_S^0 \pi^\mp}$ and $\epsilon_{5\pi}$ the corresponding reconstruction efficiencies evaluated by Monte Carlo; $b_{5\pi}$ is the background of the 5π channel.

All these numbers and the resulting annihilation frequencies are shown in the last column of Table 2. The result for the LH_2 sample is in good agreement with the bubble chamber measurement of Ref. [7].

The apparatus and trigger acceptance was studied by Monte Carlo simulation. The main distortions are due to a threshold on the charged kaon momentum around 0.18–0.20 GeV/c at the vertex. Kaons at lower momenta cannot reach the drift chamber because of energy loss. Moreover, the trigger request on the time of flight (8 ns) increases the fraction of particles with high momenta (those which reach the outer TOF barrel), thus reducing the $K_S^0\pi^\pm$ available phase space. All these effects were carefully studied and are well reproduced by our Monte Carlo. They affect only the lower corners of the Dalitz plot. We notice that, with the exception of this point, the Dalitz plot for LH_2, resembles very well the one observed in bubble chamber [1].

In Fig. 1(a)–(c) the Dalitz plots $m^2(K^\pm\pi^\mp)$ vs $m^2(K^0\pi^\mp)$, for LH_2, NTP, and LP data samples are shown.

A diagonal band around 1.3 GeV/c^2 in the $\bar{K}K$ mass is evident. The $a_0(980)$ appears as an isolated

Table 2
Annihilation frequencies

	$N_{K^\pm K_S^0 \pi^\mp}$	$N_{5\pi}$	$1 - b_{5\pi}$	$\epsilon_{K^\pm K_S^0 \pi^\mp}/\epsilon_{5\pi}$	$r_{K^\pm K_S^0 \pi^\mp}$
LH_2	10938	891400	0.91 ± 0.02	0.756 ± 0.007	$(31.6 \pm 5) \cdot 10^{-4}$
NTP	27718	1571000	0.91 ± 0.02	0.946 ± 0.013	$(36.4 \pm 5) \cdot 10^{-4}$
LP	3035	302000	0.91 ± 0.02	0.454 ± 0.007	$(43.2 \pm 6) \cdot 10^{-4}$

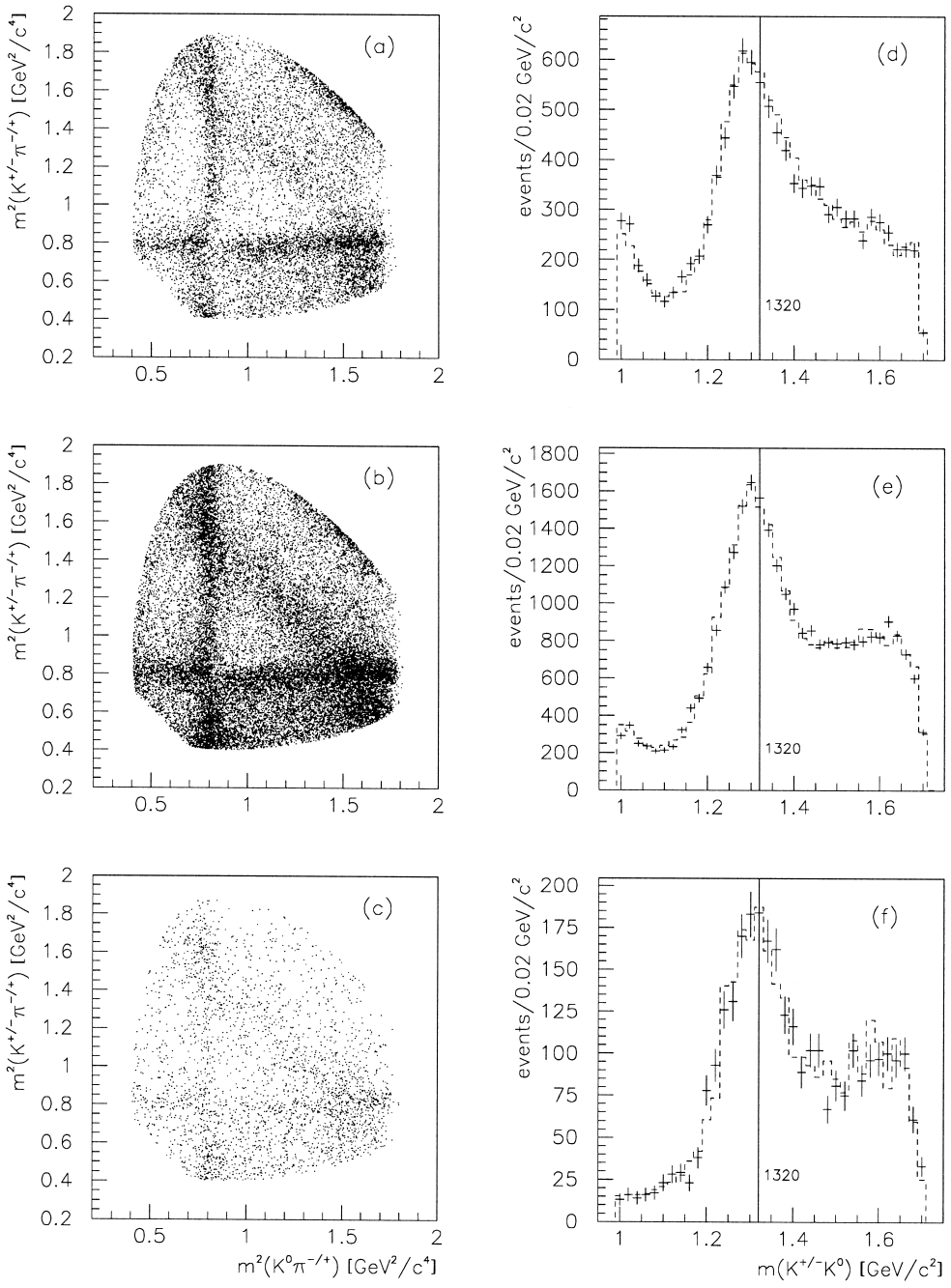

Fig. 1. (a), (b), (c): Dalitz plot of LH_2 and 5 mbar data, respectively; (d), (e), (f): $\bar{K}K$ invariant mass with superimposed the best fit of LH_2, NTP, and 5 mbar data, respectively.

band in the upper corner. Both the neutral and the charged $K^*(892)$ bands clearly appear. Interference effects, at the band crossing, appear not to be strong.

The most striking changes in the spectra, going from the liquid target to the 5 mbar one, are better emphasized in the projected $\bar{K}K$ invariant masses, as

shown in Fig. 1(d)–(f). The $a_0(980)$ signal strongly decreases going from the high to the low density target one and the peak around 1.3 GeV/c^2 shifts from ~ 1.28 to ~ 1.32 GeV/c^2 (the $a_2(1320)$ position is marked by an arrow in those figures). The position of this peak, in the LH_2 data, coincides with the one observed in bubble chamber [1]. Finally, an accumulation of events in the high $\bar{K}K$ mass region (~ 1.6 GeV/c^2) is noted as the P wave fraction increases. Such effects due partially to kinematical reflections from K^* reflections, and partially to the production of high mass states as the $\rho(1700)$.

The partial wave analysis was performed within the framework of the isobar model. The basic isobars were $a_0(980)$, $a_2(1320)$, $\rho(1700)$, $K^*(890)$, and $(K\pi)_{\text{S wave}}$. The allowed $J^{PC}(^{2S+1}L_J)$ $\bar{p}p$ states are $0^{-+}(^1S_0)$, $1^{--}(^3S_1)$, $1^{+-}(^1P_1)$, $1^{++}(^3P_1)$, and $2^{++}(^3P_2)$. In Table 3 we show for each J^{PC} initial $\bar{p}p$ state which isobars can be produced, indicating the relative orbital angular momentum l with respect to the spectator. We considered all possible reactions with $l \leq 2$. The $0^{++}(^3P_0)$ state is forbidden by selection rules. We note also that from 1^{+-} and 1^{++} exactly the same states can be produced. Thus the two contributions cannot be distinguished and we considered only one (we call it 1^+).

All resonances were described by relativistic Breit Wigner functions. The $a_0(980)$ decaying to $\bar{K}K$ can be under threshold and was parameterized by a Flattè function [8]. The analysis, repeated using the K matrix formalism [9], gave the same results. This is resonable since the K matrix formalism [9] is expected to be important only for broad and overlapping resonances.

In the $K\pi$ system, evidence of S wave interactions has been reported by many experiments. The best experimental data are from LASS and are interpreted in terms of a resonance $K_0^*(1430)$ and a smooth interaction at lower energy [10]. We tested different parameterizations using the Tornqvist model [11] or a K matrix amplitude [12].

Each reaction mode represents an elementary decay amplitude, which can be written in the form

$$A_{J^{PC},I,L,l} = \sum_{I_3} c_{I,I_3} \cdot F_{I,I_3,L} \cdot Z_{I_3,L,l} \cdot Q^l,$$

where an isospin decomposition is performed with the Clebsch-Gordan coefficients c; F is the dynamical function describing the intermediate isobar; Q is the spectator momentum and Q^l is a centrifugal barrier factor. The spin part Z of the amplitude was evaluated in the helicity formalism.

The total amplitude from a given $\bar{p}p$ J^{PC} is

$$A_{J^{PC}} = \sum_{I,L,l} x_{I,L,l} \cdot e^{i\phi_{I,L,l}} \cdot A_{J^{PC},I,L,l},$$

where x and ϕ are free parameters to be fitted from the data. Amplitudes with the same J^{PC} but different I may interfere. That is the case, for instance, of $K^*\bar{K}$, or $(K\pi)_S\bar{K}$.

The three data sets were simultaneously fitted by means of a maximum likelihood method by maximizing the function

$$L = \sum_{k=1}^{3} \ln\left(\sum_{J^{PC}} \frac{p_{k,J^{PC}} \cdot |A_{J^{PC}}|^2}{\int p_{k,J^{PC}} \cdot |A_{J^{PC}}|^2 d\Omega} \right),$$

where the first summation is over the data samples, and for each sample an incoherent sum over the J^{PC} states is performed.

The coefficients $p_{k,J^{PC}}$ are the global J^{PC} contributions for each sample and are free parameters. The amplitudes $A_{J^{PC}}$ are the same independently from

Table 3
Isobar contributions from each $J^{PC}(\bar{p}p)$

isobar state	$0^{-+}(^1S_0)$	$1^{--}(^3S_1)$	$1^+(^1P_1$ or $^3P_1)$	$2^{++}(^3P_2)$
$K^*(890)\bar{K}$ $I=0,1$	$l=1$	$l=1$	$l=0,2$	$l=2$
$(K\pi)_S\bar{K}$ $I=0,1$	$l=0$	–	$l=1$	–
$\rho(1700)\pi$	$l=1$	$l=1$	$l=0$	$l=2$
$a_2(1320)\pi$	$l=2$	$l=2$	$l=1$	$l=1$
$a_0(980)\pi$	$l=0$	–	$l=1$	–

the data set. That means that the interference pattern inside each J^{PC} state is the same for LH_2, NTP, and LP. Therefore the simultaneous fit of the three samples imposes strong constraints which would be otherwise absent performing three separate analysis.

We proceeded looking for the simplest meaningful solution.

All the contributions shown in Table 3 were included in the amplitude, but only those whose contribution corresponds to a non negligible change in the likelihood were retained in the final fit.

The annihilation frequency ${}^{\rho}r_{J^{PC}}$ of the channel from a given J^{PC} is the product of the J^{PC} $\bar{p}p$ population ${}^{\rho}f_{J^{PC}}$ at the target density ρ times the hadronic J^{PC} branching ratio $B_{J^{PC}}$. However, it has been measured by this experiment [5] that ${}^{\rho}f^{1}{}_{S_0}/{}^{\rho}f^{3}{}_{S_1}$ is independent from the target density, in agreement with the cascade model [13]. The present analysis agrees with this result; therefore the ratio $f^{1}{}_{S_0}/f^{3}{}_{S_1}$ has been kept constant, i.e. independent from the target density, in the fit presented here. Moreover, the present results for NTP and LP are consistent with the constancy of the ratio between the singlet state ${}^1P_1$ and each triplet P state separately. At LH_2, since the P wave is rather small, the NTP and LP ratio has been imposed, requiring in that manner to be constant.

The release of this condition does not imply a significant improvement of the fit, even if the number of parameters increases.

In a first attempt we tried to fit the data with $K^*(890)$, $(K\pi)_S$, $a_0(980)$, and $a_2(1320)$, excluding $\rho(1700)$, and other possible scalar states. Comparing the LH_2 results with those of the bubble chamber experiment [1] we observe some similar behaviour: K^* production from ${}^1S_0$ is dominated by $I=0$, whereas, on the contrary, its production from ${}^3S_1$ is dominated by $I=1$. However, several differences are present: P wave is not negligible in LH_2 (whereas it has been neglected in Ref. [1]) and almost all $a_2(1320)$ contribution appears to come from ${}^3P_2$ and not from ${}^1S_0$.

Overall, this first hypothesis is not able to provide a good description of our data samples ($\chi^2 > 2$).

The introduction of the $\rho(1700)$ improves significantly the fit. The likelihood changes by about 800 units, and $\chi^2 \sim 1.3$. The values of mass and width of the vector state are $m = 1.60 \pm 0.02$, $\Gamma = 0.22 \pm 0.04$ GeV/c^2 and its contribution appears to be strong. The possible presence of a second ρ state around 1.450 GeV/c^2 [6] was checked by allowing the masses of both states to move freely. In that case, since the states are broad and could overlap, the Breit-Wigner functions were replaced by a K matrix [9]. The fit provides an indication of a state around 1.4 GeV/c^2 but no firm conclusions can be drawn.

However, this data description was not considered adequate and an improvement was sought for.

Looking at Figs. 1(c)–(e) two effects are apparent. First, the suppression of $a_0(980)$ as the pressure decreases. This clearly indicates a dominant production from $\bar{p}p$ S-states, as confirmed by the fit. The second effect is the shift of the $a_2(1320)$ mass peak with respect to its nominal value as the target density increases. The fit returns $m = 1.28 \pm 0.01$. for the LH_2 data, where the error takes into account the experimental resolution. This value is clearly incompatible with the value reported by the PDG [6]. A possible interpretation would be the presence of a new scalar state with a mass lower than $a_2(1320)$, having the same production mechanism as for the $a_0(980)$.

Therefore we added to the amplitude a new scalar state in the $a_2(1320)$ mass region. This results in a consistent improvement the fit by about 160 units in the likelihood and the $\chi^2 \sim 1.1$. The values of the mass and width of the new scalar state are $m = 1.29 \pm 0.01$, $\Gamma = 0.080 \pm 0.005$ GeV/c^2.

Different choices of J^{PC} quantum numbers were also tested for that state. No evidence of 1^- states in this mass region was found whereas the 2^+ assignment gave a likelihood by 120 units worse than the 0^+ choice.

In order to exclude the possibility that the mass peak shifting could be due to the choice of $K\pi$ S wave, different parametrizations were tested for this contribution [11,12]. They lead to absolutely compatible results, indicating once again the need for a new scalar state.

Moreover, the fit was also repeated using different parametrizations of the Breit-Wigner functions and excluding the events on the Dalitz plot boundaries. The fit results remained stable.

In conclusion, our best fit solution required the contributions of $a_0(980)$, $a_0(1300)$, $a_2(1320)$, $\rho(1700)$, $K^*(890)$, and $(K\pi)_S$.

Fig. 1(d)–(f) shows the result of the best fit for the $\bar{K}K$ masses at the three densities.

A $I=1$ state around 1.45 GeV/c^2 ($a_0(1450)$) was reported by the Crystal Barrel Collaboration in the analysis of the $\eta\pi\pi$ final state [14].

Although in agreement on the $a_0(980)$ signature in its two main decay modes, $\eta\pi$ and $\bar{K}K$, the two analyses would seem to disagree substantially on the parameters of the other isovector scalar state, namely its mass and width. For this reason we decided to perform a detailed scan of the likelihood as a function of the mass and width parameters of the new $I=1$ scalar resonance. The considered intervals were: $1.2 < m < 1.6$ and $0.04 < \Gamma < 0.32$ GeV/c^2.

The result is shown in Fig. 2. Each cell represent the result of the fit with a fixed mass and width value of the $I=1$ $J^{PC}=0^{++}$ state. The likelihood function shows two well separated maxima. We will call them solution 1 and 2. Solution 1 has $m_1 = 1.29 \pm 0.01$ $\Gamma_1 = 0.09 \pm 0.01$ GeV/c^2. Solution 2 has $m_2 = 1.48 \pm 0.04$, $\Gamma_2 = 0.20 \pm 0.06$ GeV/c^2. The corresponding values of the likelihood and χ^2 are: $L_1 = 10910$, $\chi_1^2 = 1.1$, and $L_2 = 10845$, $\chi_2^2 = 1.2$, respectively.

We conclude that the first solution is to be preferred, as a likelihood difference of 65 units is considered to be significant. Moreover Fig. 2 shows a much better definition of the maximum shape in the case of the first solution.

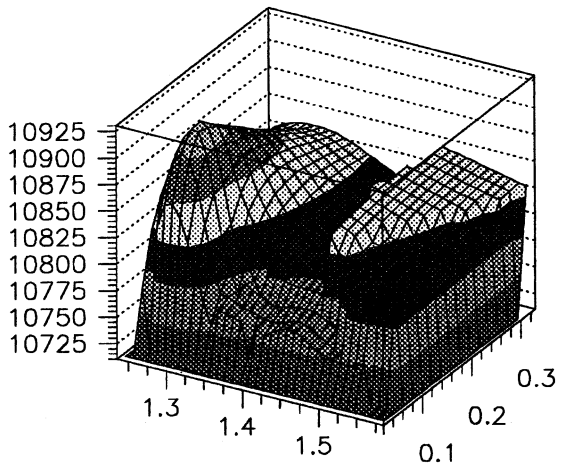

Fig. 2. Likelihood as a function of mass and width of a second scalar state.

Table 4
Single $J^{PC}(\bar{p}p)$ contributions at the three densities

$J^{PC}(\bar{p}p)\ ^{2S+1}L_J$	LH_2	NTP	LP
$0^{-+}(^1S_0)$	0.39 ± 0.03	0.17 ± 0.01	0.05 ± 0.01
$1^{--}(^3S_1)$	0.48 ± 0.03	0.20 ± 0.01	0.07 ± 0.01
Total S wave contribution	0.87 ± 0.04	0.37 ± 0.01	0.12 ± 0.01
$1^{+}(^1P_1$ or $^3P_1)$	0.08 ± 0.01	0.40 ± 0.04	0.55 ± 0.06
$2^{++}(^3P_2)$	0.05 ± 0.01	0.23 ± 0.02	0.33 ± 0.05
Total P wave contribution	0.13 ± 0.01	0.63 ± 0.04	0.88 ± 0.08

We also observe that, in case of solution 2, the scalar is produced dominantly from P-wave and not from the S-wave as expected. This point makes difficult a direct comparison with the analysis of Ref. [14] since, in that case, the P-wave contribution was neglected.

The total contributions to the channel from each $J^{PC}(\bar{p}p)$ for LH_2, NTP and LP are shown in Table 4. As one can see, at LH_2 there is a contribution of $\sim 87\%$ from S wave, and $\sim 13\%$ from P wave. At NTP we found $\sim 37\%$ from S wave, and $\sim 63\%$ from P wave. Finally, at LP, the S wave contribution is $\sim 12\%$, whereas the P wave is $\sim 88\%$. These values are in good agreement with the expectations [13].

In Table 5 the isobar contributions, evaluated neglecting the interference terms, from each $J^{PC}(\bar{p}p)$ are shown. Their sum from each $J^{PC}(\bar{p}p)$ is normalized to 1. Multiplying these numbers with those of Table 4 we can get the isobar contributions (total or from each $J^{PC}(\bar{p}p)$) at LH_2, NTP, and LP.

The $a_0(980)$ parameters are not very well established. Using the Flattè formula we found a mass $m = 0.975 \pm 0.015$ GeV/c^2, and the partial width in the $\eta\pi$ decay $\Gamma_{\eta\pi} = 0.065 \pm 0.01$ GeV/c^2. The Flattè function is rather insensitive to the value of the coupling to the $K\bar{K}$ channel, which can vary over a wide interval of values giving equally acceptable fits. It was then fixed to the $SU(3)$ value. Our results are in very good agreement with Ref. [15]. The $a_0(980)$ is produced only from singlet S wave and its contribution is $\sim 5\%$ at LH_2, 2% at NTP, practically negligible at LP. That explains why the peak

Table 5
Isobar contributions from each $J^{PC}(\bar{p}p)$ (the sum of contributions from each $J^{PC}(\bar{p}p)$ is normalized to 1)

isobar state	0^{-+} ($^1S_0$)	1^{--} ($^3S_1$)	1^{+} ($^1P_1$ or $^3P_1$)	2^{++} ($^3P_2$)
$K^*(890)\bar{K}$	0.12 ± 0.01	0.79 ± 0.02	0.46 ± 0.05	0.46 ± 0.04
$(K\pi)_S\bar{K}$	0.34 ± 0.02	–	0.11 ± 0.02	–
$\rho(1700)\pi$	0.19 ± 0.01	0.21 ± 0.01	0.34 ± 0.04	0.29 ± 0.04
$a_2(1320)\pi$	0.04 ± 0.01	0.00 ± 0.01	0.06 ± 0.02	0.25 ± 0.04
$a_0(980)\pi$	0.12 ± 0.01	–	0.00 ± 0.01	–
$a_0(1300)\pi$	0.19 ± 0.02	–	0.03 ± 0.01	–
	$\Sigma_{\text{isobar}} = 1$	$\Sigma_{\text{isobar}} = 1$	$\Sigma_{\text{isobar}} = 1$	$\Sigma_{\text{isobar}} = 1$

becomes smaller going from LH_2 to LP. These results are very stable, independently from the fit hypotheses.

The $\rho(1700)$ contribution is large, being 20 to 30% from LH_2 to LP.

Moreover, a sizeable contribution of $(K\pi)$ S wave from $\bar{p}p$ S wave is observed.

The $a_0(1300)$, is dominantly produced from S wave as for the $a_0(980)$. Its contribution is 8%, 4%, and 3% at LH_2, NTP, and LP, respectively.

The $a_2(1320)$ is more strongly produced from P wave its contribution being 3%, 9%, and 12% at LH_2, NTP and LP, respectively.

This provides a natural explanation for the systematic shift of the $K\bar{K}$ peak at the three densities.

From Table 2, the total $a_2(1320) \to \bar{K}K$ branching fraction is $(3.0 \pm 0.6) \cdot 10^{-4}$ in liquid hydrogen. This number can be compared with the same measurement performed in bubble chamber: $a_2(1320) \to \bar{K}K = (12 \pm 4) \cdot 10^{-4}$ [1].

Combining the result of Table 2 with the published values for $\bar{p}p$ annihilation into $\eta\pi\pi$ [14] and $\pi^+\pi^-\pi^+\pi^-$ [16] it is possible to obtain: $\frac{\Gamma_{a_2}(\bar{K}K)}{\Gamma_{a_2}(\eta\pi)} = 0.08 \pm 0.02$ and $\frac{\Gamma_{a_2}(\bar{K}K)}{\Gamma_{a_2}(\rho\pi)} = 0.011 \pm 0.003$. These values are to be compared with the values quoted by PDG [6]: $\frac{\Gamma_{a_2}(\bar{K}K)}{\Gamma_{a_2}(\eta\pi)} = 0.34 \pm 0.06$ and $\frac{\Gamma_{a_2}(\bar{K}K)}{\Gamma_{a_2}(\rho\pi)} = 0.070 \pm 0.012$.

In all these cases our value is definitely lower than the expected one. To evaluate the possible effect of an underestimated $a_2(1320)$ fraction additional fits were carried out by imposing an increased $a_2(1320)$ fraction. The conclusion is that the fit slowly deteriorates as the a_2 fraction increases. A reasonable fit (likelihood 10891) can still be obtained with an $a_2(1320)$ fraction increased by a factor 2. With this constraint the difference in likelihood between the hypothesis 1 is still significant (46 units).

In conclusion the fit cannot provide a meaningful solution with an $a_2(1320)$ fraction which approaches the expected values.

This discrepancy can be due to several reasons. In the data of Ref. [1] the presence of a scalar state at 1.300 GeV/c^2, although considered possible [17,18], was not taken into account in the calculation. This could have affected the evaluation of the $a_2(1320)$ rate.

In the analysis of Ref. [1,14,16] the $P-wave$ was considered to be small and was not taken in account in the analysis. This point makes the results not directly comparable.

The rates concerning $a_2(1320) \to \bar{K}K$ quoted in the PDG, come from experiments where the $a_2(1320)$ was considered the only resonant contribution in that mass region while the possible presence of an isovector scalar state, around 1.3 GeV/c^2, is suggested by the analysis of several different experiments with the same production mechanism [19–23].

It is important to stress that, in our data, the simultaneous analysis of three independent data sets, characterized by different initial angular momentum state conditions, provides strong constraints in the fit.

In particular, no ambiguity on the spin assignment of the resonant contributions in the 1.3 GeV/c^2 $\bar{K}K$ mass region is present.

The presence of $a_0(1300)$ does not affect in a sizeable way the $a_2(1320)$ fraction, which remains much lower than the calculated values even if the $a_0(1300)$ is totally neglected.

In conclusion, from the analysis of the channel $\bar{p}p \to K^{\pm}K^0_S\pi^{\mp}$ at rest,at three different target densities, we can extract three main results.

First, the evidence of a $I = 1$ scalar state in the 1.3 GeV/c^2 region which is dominantly produced from S wave.

Second, the indication of a dynamical selection rule which favours the production of $a_0(980)$ from $^1S_0$ with respect to P states. This effect shows up

clearly from the comparison of the three data sets marked by different initial $\bar{p}p$ angular momentum states.

Finally, the evidence of a massive ρ state. Our data are consistent with the presence of one ρ state around ~ 1.600 GeV$/c^2$, decaying to $\bar{K}K$, as reported by the PDG [6]. The data cannot lead to firm conclusions concerning a second ρ state around 1.4 GeV$/c^2$.

The possible presence of a scalar state in the $a_2(1320)$ mass region has been considered already in Ref. [18] within the framework of the ''*daughter trajectories*'' of Veneziano [24]. Following this theory it was pointed out that below the $a_2(1320)$ the $\eta\pi$ or $\bar{K}K$ systems could accommodate another $I=1$ $J^P=0^{++}$ resonance. Unfortunately the statistics of the available data were not sufficient to clarify the situation.

Also in $\pi^{\pm}p \to KKp(n)$ experiments at 6,7,10 and 23 GeV$/c$ [19–23] the presence of a $I=1$ scalar state around 1.3 GeV$/c^2$ was reported. In particular in Ref. [20] it was possible to fix also the isospin since the $K^-K^0_S$ decay mode was observed. However these results lacked further confirmation.

As pointed out also in Ref. [10] the 0^{++} isovector state would be expected to be close in mass to the 2^{++} $a_2(1320)$ and the 1^{++} $a_1(1260)$ and to couple strongly to $\bar{K}K$ and $\eta\pi$.

Several very recent models foresee an isovector scalar resonance in the region around 1.3 GeV$/c^2$. In a relativistic quark model with linear confinement and instanton-induced interaction [25] the isovector member of the scalar nonet is predicted at a mass of 1.32 GeV$/c^2$. This result is confirmed by the calculations based on the Nambu and Jona-Lasinio model in Ref. [26]. In Ref. [27,28] the $I=1$ state of the scalar nonet is established to be at a mass of 1.35 GeV$/c^2$ by the application of the linear mass spectrum on the basis of three mass sum rules. In the same paper [27] is pointed out that a $I=1$ 0^{++} state must exist at a mass around 1.3 GeV$/c^2$ in order to belong to the Regge trajectory on which the $\rho(1700)$ lies.

Acknowledgements

We would like to thank Prof. L. Montanet, N. Tornqvist and S. Sadovsky for helpful discussions and support, and the LEAR staff for the excellent operation of the machine.

References

[1] Conforto et al., Nucl. Phys. B 3 (1967) 469.
[2] T.B. Day, G.A. Snow, J. Sucher, Phys. Rev. 3 (1960) 864.
[3] V.G. Ableev et al., Nuovo Cimento A 107 (1994) 2279.
[4] A. Adamo et al., Sov. J. Nucl. Phys. 55 (1992) 1732.
[5] A. Bertin et al., Phys. Lett. B 385 (1996) 493.
[6] Review of particle properties, Physical review D 54 (1996) 1.
[7] R. Armenteros et al., Phys. Lett. 17 (1965) 170.
[8] S. Flattè, Phys. Lett. B 63 (1976) 224.
[9] S.U. Chung et al., Ann. Physik 4 (1995) 404.
[10] D. Aston et al., Nucl. Phys. B 296 (1988) 493.
[11] N. Tornqvist, Z. Phys. C 68 (1995) 647.
[12] A. Abele et al., Phys. Lett. B 385 (1996) 425.
[13] C.J. Batty, Nucl. Phys. A 601 (1996) 425.
[14] C. Amsler et al., Phys. Lett. B 333 (1994) 277.
[15] J.H. Lee et al., Phys. Lett. B 238 (1994) 227.
[16] A. Bertin et al., Phys. Lett. B 414 (1997) 220.
[17] R. Armenteros, B. French, $\bar{N}N$ interactions in high energy physics, vol. 4, E.H.S. Bushop (Ed.), Academic Press, New York, 1969, p. 331.
[18] L. Montanet, Proceedings Erice School, 1973, p. 511.
[19] N.M. Cason et al., Phys. Rev. Lett. 36 (1976) 1485.
[20] A.D. Martin et al., Phys. Lett. B 74 (1978) 417.
[21] Polychronakos et al., Phys. Rev. D 19 (1979) 1317.
[22] A.D. Martin, E.N. Ozmutlu, Nucl. Phys. B 158 (1979) 520.
[23] A. Etkin et al., Phys. Rev. D 25 (1982) 2446.
[24] G. Veneziano, Nuovo Cimento A 57 (1968) 190.
[25] E. Klempt et al., Phys. Lett. B 361 (1995) 160.
[26] V. Dmitrasinovic, Phys. Rev. C 53 (1996) 1383.
[27] L. Burakovsky, L.P. Horwitz, Nucl. Phys. A 609 (1996) 585.
[28] L. Burakovsky, Foundations of Physics 27 (1997) 315.